

## Article

# Role of Magnetism in Lattice Instability and Martensitic Transformation of Heusler Alloys

Ilya Razumov <sup>\*,†</sup>  and Yuri Gornostyrev <sup>\*,†</sup>

Institute of Metal Physics, Ural Branch, RAS, 620108 Ekaterinburg, Russia

\* Correspondence: rik@imp.uran.ru (I.R.); yug@imp.uran.ru (Y.G.); Tel.: +7-919-363-0548 (I.R.)

† These authors contributed equally to this work.

**Abstract:** Heusler alloys are subject of considerable interest because they exhibit a martensitic transformation (MT), a shape-memory effect and a giant magnetocaloric effect. As it is commonly believed, the pronounced magnetoelastic coupling plays a crucial role; however, the effect of alloy composition on MT is still under discussion. To describe the features of MT in  $\text{Ni}_{0.75-x}\text{Mn}_x\text{Ga}_{0.25}$  Heusler alloys, the phenomenological model that consistently considers the magnetic and lattice degrees of freedom and their mutual interplay has been developed. The magnetic entropy contribution was estimated within the framework of the microscopic approach. The proposed model allows us to describe the dependence of the martensitic transformation start temperature  $M_s(x)$  on the Mn concentration  $x$  in reasonable agreement with the experiment.

**Keywords:** Heusler alloys; martensitic transformation; magnetoelastic coupling; Bain transformation path; free energy density; ab initio parametrization

## 1. Introduction

The martensitic transformations (MT) are distinguished among the structural phase transition in solids since realized by a shear (diffusion-free) mechanism carried out by cooperative displacements of atoms [1–4]. Typically, the MT occurs during the overcooling of alloy due to lattice instability and can develop athermally at high speed. However, the MT can also be thermally activated and develop gradually, be reversible or irreversible, and lead to the formation of morphologically varied structures (see [4–7]).

MT was first discovered in iron alloys and steels as shear structural transformations from a high-temperature fcc phase ( $\gamma$ -phase, austenite) to a low-temperature bcc phase ( $\alpha$ -phase, martensite). Later it was found that similar transformations are observed in various solids, including non-magnetic shape memory alloys (NiTi, Cu-Zn-Al, Cu-Al-Ni) [3,8,9], alloys exhibiting the giant magnetocaloric effect (Gd(SiGe), (MnFe)(PAs), La-Fe-Si) [10], Heusler alloys  $\text{Ni}_{0.75-x}\text{Mn}_x\text{Z}_{0.25}$  ( $Z = \text{Al, Ga, In, Sn, Sb}$ ) [4,11,12] and so one.

Despite extensive studies [1,13–18], the physical origin of MT and its microscopic mechanisms are still under discussion as they are the result of the interplay of many factors. So, while in non-magnetic Hume–Rothery alloys [19] lattice instability is provided by electronic mechanisms [20], in iron and steel, apparently, the role of magnetism is key [21–23], and in Heusler alloys [4,24,25] both electronic and magnetic as well magnetoelastic contributions are important. In Hume–Rothery alloys below temperature  $M_s$ , a nearly second kind transformation is realized due to phonon “softening”. MT of this type can be preceded by special pretransition phenomena (“tweed structures”), the appearance of which is usually explained by the competition between elastic stresses and lattice softening [26].

In many solids, for example, in Li, Na and Cs [27], as well as in iron and steel [1], the start of martensitic transformation is possible above the temperature of absolute lattice instability, i.e.,  $M_s < T_m < T_0$ , where  $T_m$  is the transition temperature,  $T_0$  is the temperature of paraequilibrium of initial and final phases. In this case, MT show features of a first-order



**Citation:** Razumov, I.; Gornostyrev, Y. Role of Magnetism in Lattice Instability and Martensitic Transformation of Heusler Alloys. *Metals* **2023**, *13*, 843. <https://doi.org/10.3390/met13050843>

Academic Editors: João Pedro Oliveira and Ryosuke Kainuma

Received: 15 March 2023

Revised: 18 April 2023

Accepted: 23 April 2023

Published: 25 April 2023



**Copyright:** © 2023 by the authors. Licensee MDPI, Basel, Switzerland. This article is an open access article distributed under the terms and conditions of the Creative Commons Attribution (CC BY) license (<https://creativecommons.org/licenses/by/4.0/>).

phase transformation; no significant “lattice softening” is observed, and the fraction of precipitated martensite during isothermal exposure can increase with time. Wherein the nucleation of a martensitic phase requires overcoming some energy barrier whose value is comparable to  $kT$  [1,13,28].

Iron alloys belong to a special group of materials in which the high-temperature  $\gamma$ -phase is close-packed, in contrast to the low-temperature  $\alpha$ -phase. It is commonly believed that magnetism plays a decisive role in phase equilibria in iron and its alloys. Ab initio calculations [22,23] showed that the magnetic and lattice degrees of freedom are strongly coupled in  $\gamma$ -Fe, and an athermal MT scenario can be expected upon cooling below a certain critical temperature. Based on the results of these calculations and combining them with existing models [16–18], a consistent approach to describing phase transformations in iron and steel has been proposed in Refs. [23,29].

Another significant group of compounds includes Heusler alloys  $\text{Ni}_{0.75-x}\text{Mn}_x\text{Z}_{0.25}$  ( $Z = \text{Al, Ga, In, Sn, Sb}$ ). Due to pronounced magnetoelastic coupling, these alloys exhibit a martensitic transformation, a shape-memory effect, a giant magnetocaloric effect (up to  $100 \text{ J}/(\text{kg K})$ ) [12] and magnetic field induced structural reorientation phenomena [24,25,30–32]. A feature of these alloys is that both lattice and magnetic degrees of freedom contribute to structural instability. As a result, depending on the concentration of manganese, MT can be realized both above and below the Curie temperature [24,25], and when  $M_s \approx T_c$ , the lattice and magnetic contributions in MT are comparable [33,34]. This makes it possible to control the martensitic transformation by means of an external magnetic field, which is of great practical interest [11,24]. Under a magnetic field, the alloy is reversibly deformed by displacement of the boundaries of martensitic domains (which have their magnetic moments interacting with the external field), and a giant deformation (up to 10%) is achieved. When the field is turned off, elastic stresses are accommodated by restoring the original shape of the sample.

Here, we focus on the  $\text{Ni}_{0.75-x}\text{Mn}_x\text{Ga}_{0.25}$ , one of the most studied Heusler alloys [11,12,35]. In these cases, austenitic  $\gamma$ -phase has structure  $L2_1$ , which undergoes upon cooling a phase transformation into a martensitic tetragonal  $\alpha$  phase. The transformation temperature  $M_s$  depends on the Mn content (Figure 1), and several regions are distinguished on the  $M_s(x)$  dependence. According to ab initio calculations [36,37], the energy barrier on the  $\gamma \rightarrow \alpha$  MT path depends on magnetic ordering and is close to zero in the ferromagnetic state. Observable variation as the value of the hysteresis and morphology of the emerging microstructure [24,25,36] indicates a change in the shape of the transformation path with Mn concentration.

If the parent and new phases are paramagnetic ones (Mn concentration 16–18 at.%), MT occurs as a type I transformation; the martensitic phase is not modulated, and the loss mechanism is most likely related to the mobility of interfaces under applied stress [25]. In the opposite case, when both phases are ferromagnetic (Mn concentration above 21 at.%), the martensitic transformation is preceded by a “tweed structure” that undergoes a soft-mode type II martensitic transformation; the long-period M5 or M7 structure formed in the latter case appears [24,25,38]. At intermediate Mn concentration  $18 < x < 21$  at.% MT is complex since it is determined by the competition of various contributions (lattice and magnetic) to the free energy [24,25]. In this case, a characteristic plateau appears on the  $M_s(x)$  dependence (see Figure 1). This feature indicates that the magnetic ordering in the  $\alpha$ -phase promotes the martensitic transformation, while the lattice contribution determined by the features of the electronic structure remains practically the same.

There is no doubt by now that magnetism affects the MT scenario and the microstructure formation; however, the mechanism of this phenomenon remains insufficiently studied. The effect of the interaction between different order parameters (lattice, chemical, magnetic) on the MT in Heusler alloys was discussed in [25,39] using experimental data and results of first-principles calculations. Previously proposed theories of the MT in Heusler alloys [24,36,39,40] considered the elastic, magnetic and magnetoelastic contributions, as well as magnetic anisotropy and magnetostriction and lattice modulation based on Lan-

dau's phenomenological approach. As a result, a key role of magnetoelastic coupling has been revealed. However, this approach does not separate the contributions of enthalpy and entropy in the free energy, and the physical meaning of some used parameters remains undefined.

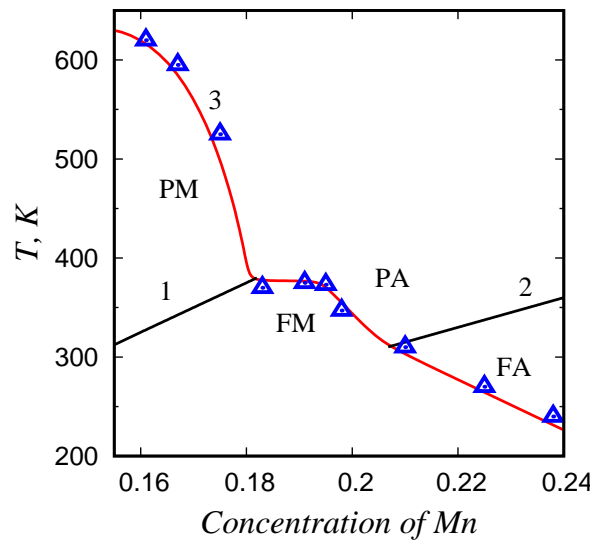


**Figure 1.** Curie temperature  $T_C^\alpha(x)$  (curve 1),  $T_C^\gamma(x)$  (curve 2) and martensitic transition temperature  $M_s$  obtained by cooling (curve 3) of the Heusler alloys  $\text{Ni}_{0.75-x}\text{Mn}_x\text{Ga}_{0.25}$  (symbols is adopted from [4]). Regions PM and PA and FM and FA correspond to paramagnetic martensite and austenite and ferromagnetic martensite and austenite, respectively.

In this paper, we generalize the existing approach for describing MT [14,15,22–24,36] to obtain the dependence  $M_s(x)$  of  $\text{Ni}_{0.75-x}\text{Mn}_x\text{Ga}_{0.25}$  alloys in a wide range of Mn concentrations. We show that variation in the shape of the curve  $M_s(x)$  when moving from region PM to region FA is due to the change in the magnetic state of the alloy. Moreover, as it follows from our calculations, the magnetoelastic contribution is insufficient to explain the plateau-like behaviour of the  $M_s(x)$  curve in the region of intermediate concentrations, and a change in the type of martensite formed should be taken into account.

## 2. Approach and Methods

### 2.1. Free Energy Density

We follow previous approaches [24,36,39,40] and consider the local density of free energy of Heusler alloy  $f(\phi, m)$  as a function of order parameters  $\phi$  and  $m = \{m_\alpha, m_\gamma\}$  that describe a lattice deformation upon  $\gamma \rightarrow \alpha$  transformation and magnetization variation, respectively. Free energy is usually written taking into account the lattice  $f_\phi(\phi, x, T)$  and magnetic  $f_m(m(x), T)$  terms as well the magnetoelastic contribution  $f_{\phi m}(\phi, m(x), T)$

$$f(\phi, m, x, T) = f_\gamma^{\text{PM}}(m_\gamma, x, T) + f_\phi(\phi, x, T) + f_m(m, x, T) + f_{\phi m}(\phi, m, x, T) \quad (1)$$

where  $f_\gamma^{\text{PM}}(m, x, T)$  is the free energy of the parent ( $\gamma$ ) phase in the paramagnetic state;  $x$  is Mn concentration and  $T$  is temperature.

Within the phenomenological approach [24,36], each contribution in Equation (1) is an expansion in powers of the order parameters. Here we use a slightly modified representation of the free energy and consider variation in the  $\gamma \rightarrow \alpha$  transformation path depending on the magnetic state. As a first step, we write the change in free energy under lattice deformation of transformation as an expansion in powers of the corresponding order parameter  $\phi$  [14,15,23]

$$f(\phi, m, x, T) = f_\gamma(m_\gamma, x, T) + 2\left(\Delta f + \frac{\lambda}{6}\right)\left(\phi^2 - \frac{\phi^4}{2}\right) + \lambda(T)\left(\frac{\phi^6}{3} - \frac{\phi^4}{2}\right), \quad (2)$$

where  $\Delta f(m, x, T) = f_\alpha(m_\alpha, x, T) - f_\gamma(m_\gamma, x, T)$  is the free energy difference of the ground states of  $\alpha$  and  $\gamma$  phases. Parameter  $\phi$  is proportional to the tetragonal deformation,  $\phi = 4\epsilon_t$ , and varies from 0 (in the  $\gamma$ -phase) to  $\pm 1$  (in the  $\alpha$ -phase). The parameter  $\lambda$  determines the height of the barrier on the Bain transformation path when the free energies of the  $\alpha$  and  $\gamma$  phases are equal. An important feature of the alloys under consideration is the dependence of  $\lambda$  on the magnetic state. As noted in the Introduction, the barrier decreases significantly upon transition to the ferromagnetic state [25,36,37]. Therefore, we accept that

$$\lambda(T) = \lambda_0 + \lambda_1(m_\alpha(T)) \quad (3)$$

Figure 2 shows schematically the dependence of ratio  $(f - f_\gamma)/f_\gamma$  on the order parameter  $\phi$  for different values of  $\Delta f$  and  $\lambda$ . Equation (2) provide the extrema of the Bain path at  $\phi = 0$  and  $\phi = \pm 1$ , and the preferred structural state is switching at  $\Delta f(x, T) = 0$ . In the case of  $\Delta f > 0$ , the  $\gamma \rightarrow \alpha$  transformation is energetically unfavourable (curve 1), and it develops barrier-free in the opposite case (curve 3) when  $-\Delta f > \lambda/6$ . When the free energies of the  $\gamma$  and  $\alpha$  phases are equal, i.e.,  $\Delta f = 0$  (curve 2), the final and initial states are separated by a barrier whose value is  $4\lambda/81$ .

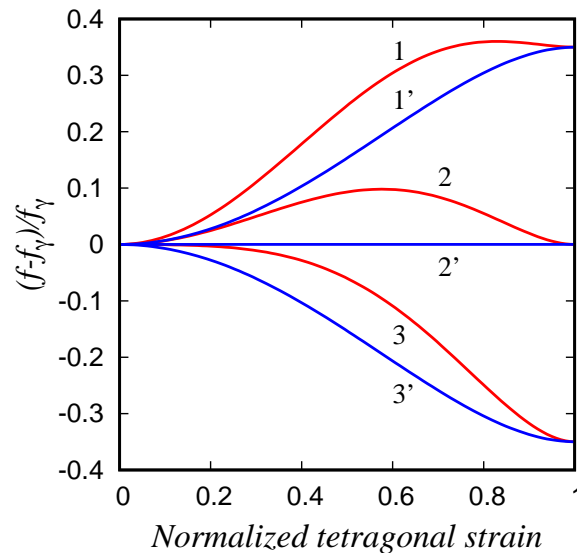


**Figure 2.** Energy variation along the transformation path determined by Equation (2).  $\Delta f/f_\gamma = 0.35$  (curves 1, 1'), 0 (curves 2, 2') and  $-0.35$  (curves 3, 3');  $\lambda/f_\gamma = 2$  (curves 1–3) and 0 (curves 1'–3').

The temperature dependence of  $f_\alpha$  and  $f_\gamma$  below Curie temperature is determined mostly by variation of the magnetisation. We write the free energy of each of the phases as an expansion in even powers of the magnetization

$$f_\gamma(x, T) - f_\gamma^{PM}(x, T) = b_\gamma^{(1)}(T - T_C^\gamma)m_\gamma^2 + b_\gamma^{(2)}m_\gamma^4 + \dots \quad (4)$$

$$f_\alpha(x, T) - f_\alpha^{PM}(x, T) = \Delta f^{PM}(x, T) + b_\alpha^{(1)}(T - T_C^\alpha)m_\alpha^2 + b_\alpha^{(2)}m_\alpha^4 + \dots \quad (5)$$

where  $\Delta f^{PM} = f_\alpha^{PM} - f_\gamma^{PM}$ ,  $T_C^{\alpha(\gamma)}$  is Curie temperature of  $\alpha(\gamma)$  phase. Substituting expressions (4) and (5) into Equation (2), we come to Equation (1) with

$$f_{\phi}(\phi, x, T) = 2\left(\phi^2 - \frac{\phi^4}{2}\right)\Delta f^{PM}(x, T) + \frac{\lambda_0}{3}(\phi^2 - 2\phi^4 + \phi^6) \quad (6)$$

$$f_m(m, x, T) = b_{\gamma}^{(1)}(T - T_C^{\gamma})m_{\gamma}^2(x, T) + b_{\gamma}^{(2)}m_{\gamma}^4(x, T) \quad (7)$$

$$f_{\phi m}(\phi, m, x, T) = 2\left(\phi^2 - \frac{\phi^4}{2}\right)\left(b_{\alpha}^{(1)}(T - T_C^{\alpha})m_{\alpha}^2 + b_{\alpha}^{(2)}m_{\alpha}^4 - b_{\gamma}^{(1)}(T - T_C^{\gamma})m_{\gamma}^2 - b_{\gamma}^{(2)}m_{\gamma}^4\right) + \frac{\lambda_1(m_{\alpha}(T))}{3}(\phi^2 - 2\phi^4 + \phi^6) \quad (8)$$

As seen from Equation (8), in line with the current assumption [24,25,36], the magnetoelastic contribution is a linear combination of terms of the form  $m^l\phi^n$ , where  $l, n$  are even. Equations (6) and (7) give the elastic and magnetic contributions in a form similar to that used previously in [36,40]. At the same time, the magnetoelastic contribution (which is usually considered for symmetry reasons) has a specific form here, taking into account the effect of magnetism on the transformation path. Note that Equation (8) differs significantly from the previously proposed model [24], where the contributions of even powers of  $\phi$  were not taken into account. We believe that our model is more correct; in particular, by virtue of its construction, it provides the correct positions of the extrema of the Bain transformation path (see Figure 2).

The free energy density (1), (6)–(8) does not take into account the contribution  $f_{el}(e_v, e_s)$  due to the dilation and trigonal deformation accompanying the transformation, which we assume here is negligibly small. We also neglect the magnetoelastic contribution like  $\phi(m_x^2 - m_y^2)$ , which is responsible for the giant deformation in Heusler alloys due to the reorientation of martensitic variants in a magnetic field [24], which is small compared to the even-degree contributions  $m^l\phi^n$  [25].

We consider some special cases to connect the parameters of the Equations (6)–(8) with observables. In the paramagnetic state (Mn concentration is less than 18%, see Figure 1), the enthalpy  $g_{\alpha(\gamma)}(x, \phi, T)$  depends on temperature even without magnetic contributions, due to the features of the electronic structure of alloy [41] leading to soft mode behaviour. As a reasonable approximation, we put

$$g_{\alpha(\gamma)}(x, \phi, T) = \tilde{g}_{\alpha(\gamma)}(x, \phi) - Tq_{\alpha(\gamma)}(x, \phi) \quad (9)$$

The free energies difference between the  $\alpha$  and  $\gamma$  phases in paramagnetic state can be represented as

$$\Delta f^{PM}(x, T) = \Delta\tilde{g}(x) - T(\Delta S(x) + \Delta q(x)) = A(x)(T - T_0^{PM}(x)), \quad (10)$$

where  $A(x) = -(\Delta S(x) + \Delta q(x))/\Omega$ ,  $\Delta\tilde{g}(x) = \tilde{g}_{\alpha}(x) - \tilde{g}_{\gamma}(x)$ ,  $\Delta q(x) = q_{\alpha}(x) - q_{\gamma}(x)$  and  $\Delta S(x) = S_{\alpha}(x) - S_{\gamma}(x)$  is entropy difference of  $\alpha$  and  $\gamma$  phases,  $T_0^{PM}$  is the temperature of paraequilibrium at which  $f_{\alpha}(x, T) = f_{\gamma}(x, T)$  and  $\Omega$  is atomic volume.

In the ferromagnetic case ( $T < T_C^{\gamma(\alpha)}$ ), the minimum free energy of the phases (Equations (4) and (5)) is reached with respect to the order parameter  $m = \{m_{\alpha}, m_{\gamma}\}$ . As a result, we obtain the temperature dependence of the magnetizations in the  $\gamma$  and  $\alpha$  phases

$$m_{\alpha(\gamma)}^2 = \frac{b_{\alpha(\gamma)}^{(1)}(T_C^{\alpha(\gamma)} - T)}{2b_{\alpha(\gamma)}^{(2)}} \quad (11)$$

Strictly speaking, Equation (11) is valid only in the vicinity of the Curie temperature. Requiring the asymptotics  $m_{\gamma(\alpha)}^2(T = 0) = 1$ , we can also rewrite this equation in the form of a reasonable approximation  $m_{\gamma(\alpha)}^2 = (T_C^{\gamma(\alpha)} - T)/T_C^{\gamma(\alpha)}$ .

## 2.2. Transformation Temperature

Realization of the martensitic transformation (MT) in the general case assumes the fulfilment of both necessary and sufficient conditions. A necessary condition for MT is the energy advantage of the  $\alpha$ -phase, i.e.,  $f_\alpha(x, T) < f_\gamma(x, T)$ . The temperature of paraequilibrium  $T_0$  arising from the condition for free energies of the  $\alpha$  and  $\gamma$  phases

$$f_\alpha(x, T_0) = f_\gamma(x, T_0) \quad (12)$$

A sufficient condition for the MT is the disappearance of the barrier on the transformation path, i.e.,

$$\frac{\partial^2 f(\phi, m, x, T)}{\partial \phi^2} \Big|_{\phi=0} \leq 0. \quad (13)$$

Condition (13) is achieved at  $T \leq M_s$  where  $M_s$  is MT start temperature.

By using relation (10) and (11) the Equations (4) and (5) can represent in the form

$$f_\gamma(x, T) - f_\gamma^{PM}(x, T) = -\tilde{b}_\gamma^{(1)}(T)(T_C^\gamma - T)^2 / (2T_C^\gamma) + \dots \quad (14)$$

$$f_\alpha(x, T) - f_\alpha^{PM}(x, T) = A(T - T_0^{PM}) - \tilde{b}_\alpha^{(1)}(T)(T_C^\alpha - T)^2 / (2T_C^\alpha) + \dots \quad (15)$$

where  $\tilde{b}_{\alpha(\gamma)}^{(1)}(T) = b_{\alpha(\gamma)}^{(1)} \theta(T_C^{\alpha(\gamma)} - T)$ , i.e., equal to zero above Curie temperature. Using the definitions (12) and (13), we obtain the following equations for temperatures  $T_0$  and  $M_s$

$$T_0 = T_0^{PM} + B_\alpha \frac{(T_C^\alpha - T_0)^2}{T_C^\alpha} - B_\gamma \frac{(T_C^\gamma - T_0)^2}{T_C^\gamma} \quad (16)$$

$$M_s = T_0^{PM} + B_\alpha \frac{(T_C^\alpha - M_s)^2}{T_C^\alpha} - B_\gamma \frac{(T_C^\gamma - M_s)^2}{T_C^\gamma} - \frac{\lambda}{6A} \quad (17)$$

where  $B_{\alpha(\gamma)} = \tilde{b}_{\alpha(\gamma)}^{(1)} / (2A)$ .

## 3. Results

### 3.1. Free Energy Parametrization

Within the considered approach, the free energy of Heusler alloys and the characteristic temperatures  $T_0$ ,  $M_s$  are determined by the Curie temperatures  $T_C^{\gamma(\alpha)}$  of  $\gamma$  and  $\alpha$  phases, the paraequilibrium temperature  $T_0^{PM}$  as well as parameters  $A$ ,  $\tilde{b}_{\alpha(\gamma)}^{(1)}$ ,  $\lambda$ . We will focus here on the effect of magnetism on temperatures  $T_0$ ,  $M_s$  and consider their behaviour as a function of Mn concentration  $x$ . Therefore, we use the experimental dependence  $M_s(x)$  in the paramagnetic region ( $x < 18\%$ , see Figure 1) and derive the  $M_s(x)$  in the ferromagnetic one; while we accept that the temperatures  $M_s(x)$  and  $T_0^{PM}$  are related by the Equation (20) in paramagnetic case.

For numerical analysis of Equations (16) and (17), we use known experimental dependence Curie temperatures on the concentration of Mn,  $T_C^{\gamma(\alpha)} = T_C^{\gamma(\alpha)}(x)$  [25]. When estimating the parameter  $A(x) = -(\Delta S(x) + \Delta q(x)) / \Omega$  ( $\Omega$  is atomic volume), we assumed that the value of  $q$  can be neglected and accept the value of the vibrational entropy variation  $\Delta S$  obtained as a result of first-principles calculations [42],  $\Delta S(x) \approx -0.24k$  where  $k$  is Boltzmann's constant.

Available experimental data (see, in particular, Ref. [25]) indicate that the transformation hysteresis and, therefore, the barrier on the transformation path decreases significantly in the ferromagnetic state when Mn concentration  $x > 21\%$ . This conclusion is also consistent with the results of ab initio calculations of Bain path energetics of considered alloys [36,37]. Note, a similar effect of magnetism was discussed earlier [23,29] in connection with the problem of  $\gamma \rightarrow \alpha$  transformation in iron. Such variation in transformation

barrier corresponds to lowering the parameter  $\lambda$ . To describe this behaviour of  $\lambda$ , we take the following approximation

$$\lambda = \lambda_0 / (1 + \zeta m_\alpha^2) \quad (18)$$

where  $\lambda_0$  and  $\zeta$  are some fitting parameters. As follows from Equations (16) and (17), the parameter  $\lambda_0$  determines the temperature difference  $T_0 - M_s$  in the paramagnetic state, and the parameter  $\zeta$  characterizes the effect of magnetism on magnitude  $T_0 - M_s$ . It should be noted that the value of  $T_0 - M_s$  is associated with the hysteresis of transformation because the reverse transformation during heating cannot occur before the necessary condition  $T > T_0$  is reached. Note, the true value of the hysteresis is determined not only by  $T_0 - M_s$  but also by other contributions (see discussion in Ref. [43]) not taken into account in our model. Such contributions can be related to pinning interface boundaries and/or accommodation processes due to microstructure reconstruction. Since we are considering alloys with thermo-elastic transformation, these contributions can be neglected. We choose the  $\lambda_0$  values to provide the value of  $T_0 - M_s$  is either 200 K or 30 K in the paramagnetic state. The first of them is typical for transformations with a large hysteresis (for example, transformation in steel), while the second is typical for the shape memory alloys under consideration.

In the framework of the phenomenological approach, the coefficients  $\tilde{b}_{\alpha(\gamma)}^{(1)}$  are fitting parameters. To estimate them, we express the magnetic enthalpy regarding exchange interactions. According to the results of ab initio calculations [36,42], the magnetic moment in the  $\text{Ni}_{0.75-x}\text{Mn}_x\text{Zr}_{0.25}$  alloy is localized mainly on Mn atoms, and its value is an order of magnitude greater than on Ni atoms. Therefore, the concentration dependence of the Curie temperatures  $T_c^{\gamma(\alpha)}(x)$  is determined primarily by the change in the concentration of Mn, and the main contribution to the magnetic energy of the alloy comes from ferromagnetic exchange interactions Mn-Ni.

Here we restrict ourselves to a simple description of magnetic interactions, using the effective exchange constants  $J_{\gamma(\alpha)}(x)$ , which provide the experimentally known Curie temperatures  $T_c^{\gamma(\alpha)}(x)$ ; wherein it is assumed that the magnetic moments of atoms of all sorts are the same. Taking into account exchange interactions only in the first coordination sphere, we write

$$J_{\gamma(\alpha)}(x) = z \sum_{i,j} c_i c_j^{(i)} J_{\gamma(\alpha)}^{(ij)}(x) \quad (19)$$

where  $z$  is the coordination number,  $c_i$  is the concentration of atoms of type  $i$ ,  $c_j^{(i)}$  is the concentration of atoms of type  $j$  on the first coordination sphere of atoms of type  $i$ ,  $J_{\gamma(\alpha)}^{(ij)}$  is the exchange energy between  $i$  and  $j$  type atoms in the  $\gamma(\alpha)$  phase.

Neglecting all exchange interactions except Mn-Ni, we get  $J_{\gamma(\alpha)}(x) = z J_{\gamma(\alpha)}^{(MnNi)}(x)/2$ . Using the approach proposed in [44] and taking into account the values of spins ( $s_{Mn} = 5/2$ ,  $s_{Ni} = 1$ ), we obtain an estimate of the effective exchange energy in terms of the Curie temperature,  $J_{\gamma(\alpha)}(x) \approx 0.63kT_c^{\gamma(\alpha)}(x)/\Omega$ . The free energy of the alloy within the framework of the microscopic approach in the effective exchange energy  $J_{\gamma(\alpha)}$  approximation is given in Appendix A. At  $T = 0\text{K}$ , in Equations (A1) and (A2) should be take  $Q_{\alpha(\gamma)} = 1$ , which makes it possible to compare with the Equations (14) and (15), which implies  $b_{\alpha(\gamma)}^{(1)} \approx 1.26k/\Omega$ ,  $B_{\alpha(\gamma)} = b_{\alpha(\gamma)}^{(1)}/2A \approx 2.6$ .

### 3.2. Results of Calculations

Let us first consider special cases corresponding to the paramagnetic and ferromagnetic states of alloy. As follows from the Equations (16) and (17), in the paramagnetic case when  $T > T_C^{\alpha(\gamma)}$  and  $B_{\alpha(\gamma)} = 0$

$$T_0 = T_0^{PM}, \quad M_s = T_0^{PM} - \lambda/6A, \quad (20)$$

i.e., the temperature  $M_s$  is shifted relative to  $T_0$  by the value  $\lambda/6A$ . In opposite case, when  $T \ll T_C^{\alpha(\gamma)}$ , from the Equations (16) and (17) we have

$$T_0 = T_0^{PM} + B(T_C^\alpha - T_C^\gamma), \quad M_s = T_0^{PM} + B(T_C^\alpha - T_C^\gamma) - \lambda/6A \quad (21)$$

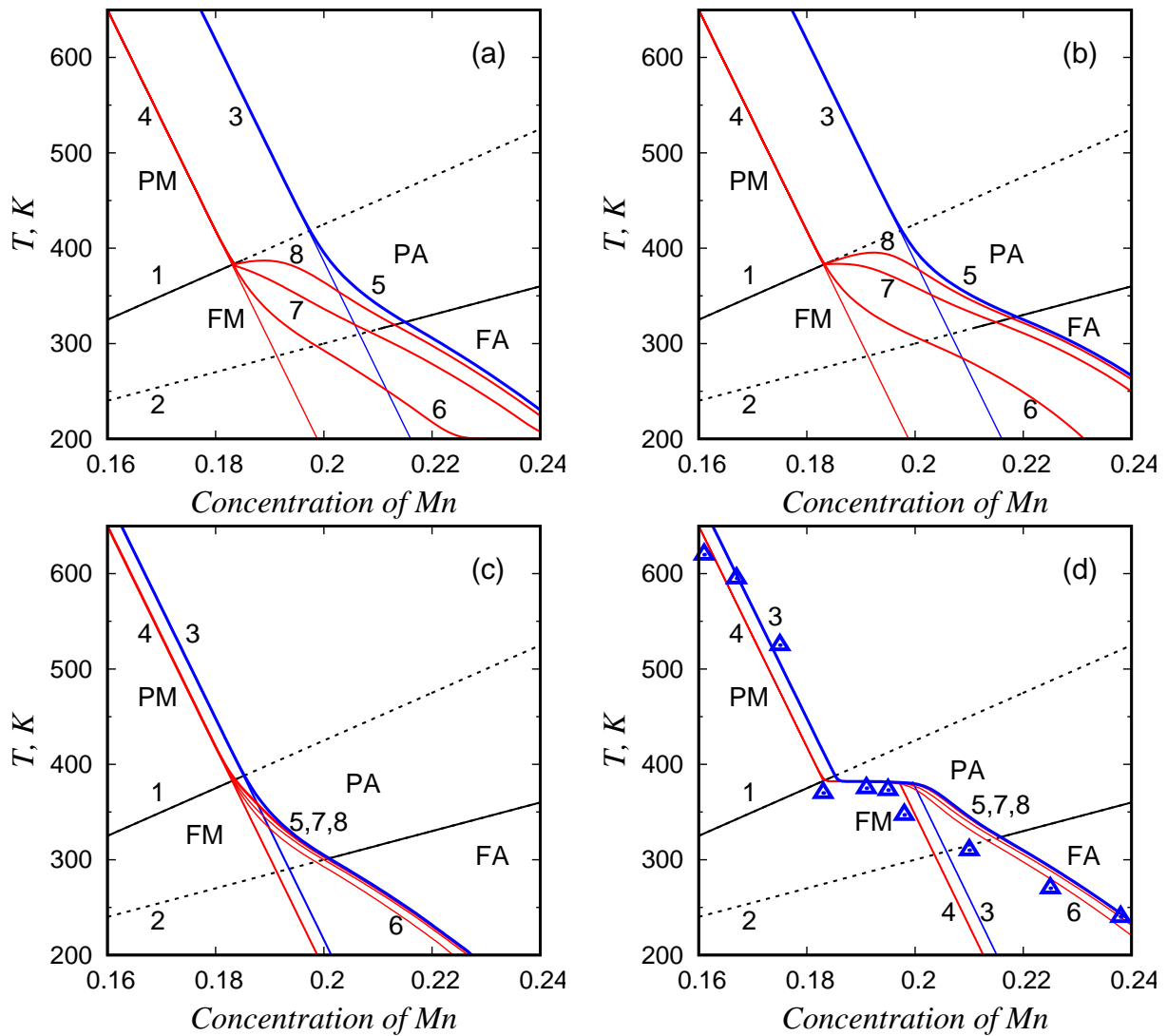
where  $B = B_\alpha = B_\gamma$  (see Section 3.1) and  $\lambda$  is approaching to zero. Thus, the transition to a ferromagnetic state will lead to an increase in the magnitude of the  $T_0$  and  $M_s$ . Note that the effect of magnetism on the temperatures  $T_0$  and  $M_s$  is due exclusively to the magnetoelastic contribution (8). Indeed, if we take  $f_{\phi m} = 0$ , from (1), (6)–(8), (12) and (13) we will obtain temperatures  $T_0$ ,  $M_s$  coinciding with the paramagnetic case (20).

Figure 3a shows the curves  $T_0(x)$ ,  $M_s(x)$  for  $\text{Ni}_{0.75-x}\text{Mn}_x\text{Ga}_{0.25}$  alloy obtained as results of numerical calculations by using Equations (16) and (17) with parameters described in Section 3.1 for the case of a large value of  $T_0 - M_s$  in the paramagnetic case. Curves 1 and 2 show the known from the experiment Curie temperatures  $T_C^\alpha(x)$ ,  $T_C^\gamma(x)$  in dependence on Mn concentration. Curves 3 and 4 describe dependences  $T_0(x)$  and  $M_s(x)$  in the paramagnetic state (line 4 was fitted to experiment). It can be seen that the transition to the ferromagnetic state with increasing Mn concentration leads to a change in the slope of the curves  $T_0(x)$  and  $M_s(x)$ . This behaviour is not surprising and is consistent with the observed in the experiment (see Figure 1) as well indicates that magnetism contributes essentially to the martensitic transformation.

The shape of the curve  $M_s(x)$  in the ferromagnetic state (6,7,8) is very sensitive to the choice of the parameter  $\zeta$ . An increase in the  $\zeta$  value leads to the appearance of a convex part on  $M_s(x)$  curve in the interval  $T_C^\gamma < M_s < T_C^\alpha$ . Thus, both a decrease in the free energy and the transformation barrier height in the ferromagnetic state leads to an increase in  $M_s(x)$ .

The phenomenological approach discussed here is physically transparent but contains a rough approximations and does not separate enthalpy and entropy contributions. Moreover, the used temperature dependence of the magnetisation (11) is too rough. More consistent is the microscopic model used in Refs. [23,29], where the magnetization is calculated using the effective Weiss field, and the magnetic entropy is taken into account using the Gelman–Feynman theorem. Here we use such an approach for a more consistent description of the martensitic transformation in the  $\text{Ni}_{0.75-x}\text{Mn}_x\text{Ga}_{0.25}$  alloy. The main Equations of the microscopic model are given in Appendix A, and the corresponding results of calculations are shown in Figure 3b. It can be seen that the curves  $M_s(x)$ ,  $T_0(x)$  calculated using the microscopic model are similar to those obtained within the phenomenological approach. For the appearance of a convex region on the curve  $M_s(x)$  in the interval  $T_C^\gamma < M_s < T_C^\alpha$ , the assumption that the parameter  $\lambda$  depends on the magnetization is still necessary. At the same time, the plateau on the curve  $M_s(x)$  is realized at a somewhat smaller value of  $\zeta$  than in Figure 3a.

Figure 3a,b describes the MT in an alloy with a large hysteresis, while a small transformation hysteresis is typical for shape memory alloys. The transformation diagram calculated for this case ( $\lambda/(6A) = 30\text{K}$ ), is shown in Figure 3c. Within the considered simple model with one type of martensite, the curves  $T_0(x)$  and  $M_s(x)$  change their slope practically immediately after crossing the Curie temperature  $T_C^\alpha(x)$ ; it does not correspond to the typical dependencies  $M_s(x)$  presented in Figure 1.



**Figure 3.** Calculated diagram of transformations of  $\text{Ni}_{0.75-x}\text{Mn}_x\text{Ga}_{0.25}$  Heusler alloys, obtained within the framework of the phenomenological model (a,c,d) and using the microscopic approach (b). Curves 1 and 2 give experimental Curie temperatures  $T_C^\alpha(x)$  and  $T_C^\gamma(x)$  in dependence on the concentration of Mn (dashed lines are extrapolation to the metastable region). Curves 3 and 4 correspond  $T_0(x)$  and  $M_s(x)$  without magnetic contribution for  $\lambda/(6A) = 200$  K (a,b) and  $\lambda/(6A) = 30$  K (c,d). Curves 5, 6, 7 and 8 correspond  $T_0(x)$  and  $M_s(x)$  when magnetism is taken into account,  $B_\alpha(0) = B_\gamma(0) = 2.6$ . Curves 6, 7 and 8 were obtained for  $\zeta = 0$ ,  $\zeta = 5$  and  $\zeta = 25$ , respectively. Triangles correspond to experimental data from [4]. Only one type of martensite was considered in cases (a–c), and the formation of a modulated state was taken into account in case (d); the parameter  $P_0/A$  was chosen equal to 180K.

For a more consistent description of the  $T_0(x)$  and  $M_s(x)$  behaviour in the region where Mn concentrations above 18 at%, we must take into account that ferromagnetic martensite is characterized by greater tetragonality  $c/a$  [4,33] and accompanied by the formation of modulated 5M/7M structures [34]. The formation of a modulated state occurs primarily for electronic instability of the austenite (see Ref. [45]) and results in a decrease in the free energy of the alloy. To take into account such a change in the energy of martensite, we make the following substitution in Equation (5)

$$f_\alpha \rightarrow f_\alpha - P_0\theta(T_s - T), \quad (22)$$

where  $\theta(T)$  is Heaviside function,  $T_s$  is temperature corresponding to the intersection point of the curves  $T_C^\alpha(x)$  and  $M_s(x)$ ,  $P_0$  is parameter. As follows from Equations (12) and (13), such a correction of  $f_\alpha$  leads to the appearance an additional term  $P_0\theta(T_s - T)/A$  on the right side of Equations (16) and (17)

$$T_0 = T_0^{PM} + B_\alpha \frac{(T_C^\alpha - T_0)^2}{T_C^\alpha} - B_\gamma \frac{(T_C^\gamma - T_0)^2}{T_C^\gamma} + \frac{P_0\theta(T_s - T_0)}{A} \quad (23)$$

$$M_s = T_0^{PM} + B_\alpha \frac{(T_C^\alpha - M_s)^2}{T_C^\alpha} - B_\gamma \frac{(T_C^\gamma - M_s)^2}{T_C^\gamma} - \frac{\lambda}{6A} + \frac{P_0\theta(T_s - M_s)}{A} \quad (24)$$

As it is seen from Equations (23) and (24), the curves  $T_0(x)$ ,  $M_s(x)$  for the paramagnetic state of modulated 5M/7M martensite can be obtained by shifting up the corresponding curves of unmodulated martensite L1<sub>0</sub> by  $P_0/A$ . In this case, the switching of the preferred state of martensite is realized when cooling to the temperature  $T_s$  and is associated with the appearance of magnetization in  $\alpha$ -phase. The numerical solution of Equations (23) and (24) taking into account magnetic contributions is shown in Figure 3d. Good agreement of the calculated curve  $M_s(x)$  and experimental data are ensured by choosing  $P_0/A = 180$  K (i.e.,  $P_0 \approx 0.004$  eV/at). In this case, the curve  $M_s(x)$  shifts to the right by the  $\Delta x \sim 2$  at.%.

Thus, the role of magnetism in the considered phenomenological model turns out to be dual. On the one hand, when cooled to a temperature  $T_s$ , magnetism provokes the formation of 5M/7M martensite, which leads to the appearance of a plateau on the  $T_0(x)$ ,  $M_s(x)$  curves. On the other hand, below the temperature  $T_C^\alpha(x)$ , the magnetic contribution leads to a change in the slope of these curves (c.f. curves 5–8 and 3, 4 in Figure 3d).

#### 4. Discussion

A model of martensitic transformation in Ni<sub>0.75-x</sub>Mn<sub>x</sub>Ga<sub>0.25</sub> Heusler alloys, which consistently considers the magnetic and lattice degrees of freedom as well as the magnetoelastic contribution, has been developed. This model generalizes the previously proposed approaches [24,36,39,40] and considers the effect of magnetism on the transformation path. The proposed model allows the revealing of the important role of magnetism in martensitic transformation, which leads to a change in the mechanism of transformation and temperature  $M_s(x)$  with an increase in the Mn concentration.

It is shown that magnetism leads to a change in the slope of both paraequilibrium curves  $T_0(x)$  and martensitic start temperatures curves  $M_s(x)$  in the ferromagnetic region; it is due exclusively to the magnetoelastic contribution (8). The effect of magnetism on the curve  $T_0(x)$ , which is determined by condition (12), is due to a decrease in the free energy of the ferromagnetic state and is determined by the mismatch of the Curie temperatures,  $T_C^\alpha$  and  $T_C^\gamma$ . At the same time, the effect of magnetism on the  $M_s(x)$  curve, which is defined by condition (13), turns out to be more complicated since it is caused both by the dependence on the magnetism of the free energy of  $\gamma$  and  $\alpha$  phases as well by a change in the height of the transformation barrier.

The parametrization of the proposed model was carried out using experimental data and estimates within the microscopic approach. In particular, we used a linear approximation of experimental data to determine the functions  $T_C^\alpha(x)$ ,  $T_C^\gamma(x)$  and  $T_0^{PM}(x)$  in dependence on Mn concentration  $x$ . It made possible to calculate the temperatures  $T_0(x)$ ,  $M_s(x)$  in reasonable agreement with the experiment (Figure 3). At the same time, the behaviour in the plateau region significantly depends on the value of the parameter  $\zeta$  and  $P_0$ , the choice of which lies beyond the developed model approach. We believe that the main reason for the anomalous plateau of the curve  $M_s(x)$  in the range of intermediate Mn concentrations (0.18–0.20 at%) is a change in the type of martensite formed, which is accompanied by a variation in the free energy by  $P_0$ . It should be noted that the use of the microscopic approach (Appendix A) gives a more reliable description  $T_0(x)$ ,  $M_s(x)$  in the range of intermediate concentrations (compare Figure 3a and Figure 3b).

The phenomenological approach used contains a number of rather rough approximations. In particular, the  $B_{\alpha(\gamma)}$  parameters were estimated by neglecting all exchange interactions except for Mn–Ni on the first coordination sphere, dependence  $M_s(x)$  in the absence of magnetism is approximated by a linear function and extrapolated to the region of high concentrations (curve 4 in Figure 3), the Bain path energetics are taken in a rather particular form. Nevertheless, the proposed model makes it possible to describe quite consistently the main features of the observed dependence of the martensitic transformation temperature  $M_s(x)$  on the composition of  $\text{Ni}_{0.75-x}\text{Mn}_x\text{Ga}_{0.25}$  alloys. Although the proposed model does not take into account the features of microstructure formation, it is quite general and can be used to describe the role of magnetism in the development of lattice instability and martensitic transformation in other Heusler alloys.

## 5. Conclusions

The Landau-type phenomenological model that consistently considers the magnetic and lattice degrees of freedom, including the magnetoelastic coupling, has been developed. The considered approach differs from those proposed earlier, considering the effect of magnetism on the transformation path. The parametrization of the proposed model was carried out using experimental data and estimates within the microscopic approach. The considered model allows to describe the concentration dependence of the martensitic start temperature  $M_s(x)$  of  $\text{Ni}_{0.75-x}\text{Mn}_x\text{Ga}_{0.25}$  alloys in reasonable agreement with the experiment. We have shown that (i) the proposed model allows you to correctly describe the change in the slope of the curves  $M_s(x)$  and  $T_0(x)$  upon the passage to the ferromagnetic state of alloy and (ii) to explain an anomalous behaviour (plateau) of  $M_s(x)$  and  $T_0(x)$  curves in the region of intermediate concentrations of Mn ( $0.19 < x < 0.20$ ), the formation of modulated martensite with lower energy must be taken into account.

**Author Contributions:** Conceptualization, funding acquisition, project administration, supervision, data curation, validation, writing—review, editing, translation, Y.G.; formal analysis, investigation, methodology, resources, software, visualization, writing—original draft preparation, I.R. All authors have read and agreed to the published version of the manuscript.

**Funding:** The research was carried out within the state assignment of the Ministry of Science and Higher Education of the Russian Federation (topic Structure, No. AAA-A18-118020190116-6).

**Conflicts of Interest:** The authors declare no conflict of interest. The funders had no role in the design of the study; in the collection, analyses, or interpretation of data; in the writing of the manuscript; or in the decision to publish the results.

## Abbreviations

The following abbreviations are used in this manuscript:

MT	Martensitic transformation
PM	Paramagnetic martensite
PA	Paramagnetic austenite
FM	Ferromagnetic martensite
FA	Ferromagnetic austenite

## Appendix A. Microscopic Approach

Within the considered simple model, the magnetic moments of atoms of all sorts are assuming the same and effective exchange interactions are determined by Equation (19). In this approximation, the magnetic contribution to the free energy can be presented as the sum of the contributions associated with the exchange energy and magnetic entropy

$$f_{\gamma}(x, T) - f_{\gamma}^{PM}(x, T) = -J_{\gamma}(x)Q_{\gamma}(x, T) - TS_{\gamma}^m \quad (\text{A1})$$

$$f_{\alpha}(x, T) - f_{\alpha}^{PM}(x, T) = A(T - T_0^{PM}) - J_{\alpha}(x)Q_{\alpha}(x, T) - TS_{\alpha}^m \quad (\text{A2})$$

where  $Q_{\alpha(\gamma)} = \langle s_0^{\alpha(\gamma)} s_1^{\alpha(\gamma)} \rangle / s^2$  is correlation function of interacting spins,  $S_{\gamma(\alpha)}^m$  is the magnetic entropy. In the limiting case  $T = 0\text{K}$  we have  $Q_{\alpha(\gamma)} = 1$  and

$$f_{\gamma}(x, 0) - f_{\gamma}^{PM}(x, 0) = -J_{\gamma}(x) \quad (\text{A3})$$

$$f_{\alpha}(x, 0) - f_{\gamma}^{PM}(x, 0) = -AT_0^{PM}(x) - J_{\alpha}(x) \quad (\text{A4})$$

As in the previous paper [23], to calculate the magnetic contribution to the free energy, we use the Gelman–Feynman theorem. Then the Equations (A1) and (A2) take the form

$$f_{\gamma}(x, T) - f_{\gamma}^{PM}(x, T) = - \int_0^{J_{\gamma}(x)} Q_{\gamma}(J_{\gamma}(x), T) dJ_{\gamma} \quad (\text{A5})$$

$$f_{\alpha}(x, T) - f_{\gamma}^{PM}(x, T) = A(T - T_0^{PM}) - \int_0^{J_{\alpha}(x)} Q_{\alpha}(J_{\alpha}(x), T) dJ_{\alpha} \quad (\text{A6})$$

Equations (A5) and (A6) take into account both magnetic enthalpy and magnetic entropy contributions. Using these equations, we obtain (instead of (16) and (17)) the following expressions for temperatures  $T_0$  and  $M_s$ :

$$T_0 = T_0^{PM} + B \left( \int_0^{T_c^{\alpha}} Q_{\alpha}(T_c^{\alpha}, T_0) dT_c^{\alpha} - \int_0^{T_c^{\gamma}} Q_{\gamma}(T_c^{\gamma}, T_0) dT_c^{\gamma} \right) \quad (\text{A7})$$

$$M_s = T_0^{PM} + B \left( \int_0^{T_c^{\alpha}} Q_{\alpha}(T_c^{\alpha}, M_s) dT_c^{\alpha} - \int_0^{T_c^{\gamma}} Q_{\gamma}(T_c^{\gamma}, M_s) dT_c^{\gamma} \right) - \lambda(M_s) / (6A) \quad (\text{A8})$$

Within the considered simple model, we do not take into account the differences between short-range and long-range magnetic order, and the interaction of each magnetic moment with the rest of the crystal is replaced by the action of the effective Weiss field. Since the temperature dependence of the magnetization has a similar form for different values of the spin [46], we use the expression  $m(T)$ , which is valid for the spin 1/2

$$m_{\alpha(\gamma)} = th \left( \frac{m_{\alpha(\gamma)} T_C^{\alpha(\gamma)}}{T} \right) \quad (\text{A9})$$

The temperatures  $T_0$ ,  $M_s$  can be found as a result of the numerical solution of the integral Equations (A7) and (A8) with the correlation function  $Q_{\alpha(\gamma)} = m_{\alpha(\gamma)}^2$ , defined by the Equation (A9).

## References

1. Kurdyumov, G.V.; Utevskii, L.M.; Entin, R.I. *Prevrashcheniya V Zheleze I Stali (Transformations Iron Steel)*; Nauk: Moscow, Russia, 1977; 236p. (In Russian)
2. Nishiyama, Z. *Martensitic Transformation*; Academic Press: New York, NY, USA, 1978; 480p.
3. Middleton, L.A.; Kennon, N.; Dunne, D. Martensitic transformation in nitinol. *Metallography* **1985**, *18*, 61–72. [[CrossRef](#)]
4. Buchel'nikov, V.D.; Vasil'ev, A.N.; Koledov, V.V.; Taskaev, S.V.; Khovailo, V.V.; Shavrov, V.G. Magnetic shape-memory alloys: Phase transitions and functional properties. *Phys. Usp.* **2006**, *49*, 871–877. [[CrossRef](#)]
5. Zuo, X.; Zhang, W.; Chen, Y.; Oliveira, J.P.; Zeng, Z.; Li, Y.; Luo, Z.; Ao, S. Wire-based directed energy deposition of NiTiTa shape memory alloys: Microstructure, phase transformation, electrochemistry, X-ray visibility and mechanical properties. *Addit. Manuf.* **2022**, *59*, 103115. [[CrossRef](#)]
6. Teshome, F.B.; Peng, B.; Oliveira, J.P.; Shen, J.; Ao, S.; Li, H.; Chen, L.; Tan, C.; Song, X.; Zhou, N.; et al. Role of Pd interlayer on NiTi to Ti6Al4V laser welded joints: Microstructural evolution and strengthening mechanisms. *Mater. Des.* **2023**, *228*, 111845. [[CrossRef](#)]
7. Li, B.; Wang, L.; Wang, B.; Li, D.; Oliveira, J.P.; Cui, R.; Yu, J.; Luo, L.; Chen, R.; Su, Y.; et al. Electron beam freeform fabrication of NiTi shape memory alloys: Crystallography, martensitic transformation, and functional response. *Mater. Sci. Eng. A* **2022**, *843*, 143135. [[CrossRef](#)]

8. Lagoudas, D.C.; Hartl, D.J. Aerospace applications of shape memory alloys. *Proceedings of the Institution of Mechanical Engineers, Part G. J. Aerosp. Eng.* **2007**, *221*, 535–552.
9. Song, G.; Ma, N.; Li, H.-N. Applications of shape memory alloys in civil structures. *Eng. Struct.* **2006**, *28*, 1266–1274. [[CrossRef](#)]
10. Gschneidner, K.A., Jr.; Pecharsky, V.K.; Tsokol, A.O. Recent developments in magnetocaloric materials. *Rep. Prog. Phys.* **2005**, *68*, 1479–1539. [[CrossRef](#)]
11. Tavares, S.; Yang, K.; Meyers, M.A. Heusler alloys: Past, properties, new alloys, and prospects. *Prog. Mater. Sci.* **2023**, *132*, 101017. [[CrossRef](#)]
12. Bachagha, T.; Sunol J. All-d-Metal Heusler Alloys: A Review. *Metals* **2023**, *13*, 111. [[CrossRef](#)]
13. Cohen, M.; Machlin, E.S.; Paranjpe, V.G. Thermodynamics of the Martensitic Transformation. In *Thermodynamics in Physical Metallurgy*; American Society of Metals: Cleveland, OH, USA, 1950; p. 242.
14. Barsch, G.R.; Krumhansl, J.A. Twin Boundaries in Ferroelastic Media without Interface Dislocations. *Phys. Rev. Lett.* **1984**, *53*, 1069–1072. [[CrossRef](#)]
15. Krumhansl, J.A.; Gooding, R.J. Structural phase transitions with little phonon softening and first-order character. *Phys. Rev. B* **1989**, *39*, 3047–3056. [[CrossRef](#)] [[PubMed](#)]
16. Rasmussen, K.O.; Lookman, T.; Saxena, A.; Bishop, A.R.; Albers, R.C.; Shenoy, S.R. Three-Dimensional Elastic Compatibility and Varieties of Twins in Martensites. *Phys. Rev. Lett.* **2001**, *87*, 055704. [[CrossRef](#)] [[PubMed](#)]
17. Shenoy, S.R.; Lookman, T.; Saxena, A.; Bishop, A.R. Martensitic textures: Multiscale consequences of elastic compatibility. *Phys. Rev. B* **1999**, *60*, R12537. [[CrossRef](#)]
18. Bouville, M.; Ahluwalia, R. Interplay between Diffusive and Displacive Phase Transformations: Time-Temperature-Transformation Diagrams and Microstructures. *Phys. Rev. Lett.* **2006**, *97*, 055701. [[CrossRef](#)] [[PubMed](#)]
19. Hume-Rothery W. Properties and Conditions of Formation of Intermetallic Compounds. *J. Inst. Met.* **1926**, *35*, 295–361.
20. Katsnelson, M.I.; Naumov, I.; Trefilov A.V. Singularities of the electronic structure and premartensitic anomalies of lattice properties in beta-phases of metals and alloys. *Phase Transit.* **1994**, *49*, 143–191. [[CrossRef](#)]
21. Okatov, S.V.; Kuznetsov, A.R.; Gornostyrev, Y.N.; Urtsev, V.N.; Katsnelson, M.I. Effect of magnetic state on the  $\gamma$ - $\alpha$  transition in iron: First-principles calculations of the Bain transformation path. *Phys. Rev. B* **2009**, *79*, 094111. [[CrossRef](#)]
22. Okatov, S.V.; Gornostyrev, Y.N.; Lichtenstein, A.I.; Katsnelson, M.I. Magnetoelastic coupling in  $\gamma$ -iron. *Phys. Rev. B* **2011**, *84*, 214422. [[CrossRef](#)]
23. Razumov, I.K.; Boukhvalov, D.V.; Petrik, M.V.; Urtsev, V.N.; Shmakov, A.V.; Katsnelson, M.I.; Gornostyrev Y.N. Role of magnetic degrees of freedom in a scenario of phase transformations in steel. *Phys. Rev. B* **2014**, *90*, 094101. [[CrossRef](#)]
24. Vasil'ev, A.N.; Buchel'nikov, V.D.; Takagi, T.; Khovailo, V.V.; Estrin, E.I. Shape memory ferromagnets. *Phys. Usp.* **2003**, *46*, 559–588. [[CrossRef](#)]
25. Mejia, C.S.; Born, N.-O.; Schiemer, J.A.; Felser, C.; Carpenter, M.A.; Nicklas, M. Strain and order-parameter coupling in Ni-Mn-Ga Heusler alloys from resonant ultrasound spectroscopy. *Phys. Rev. B* **2018**, *97*, 094410. [[CrossRef](#)]
26. Kartha, S.; Krumhansl, J.A.; Sethna, J.P.; Wickham, L.K. Disorder-driven pretransitional tweed pattern in martensitic transformations. *Phys. Rev. B* **1995**, *52*, 803–822. [[CrossRef](#)] [[PubMed](#)]
27. Smith, H.G.; Berliner, R.; Trivisonno, J. Neutron Scattering Studies of the Structure and Lattice Dynamics of the Alkali Metals. In *Proceedings of the International Conference on Martensitic Transformations (ICOMAT-92)*, Monterey, CA, USA, 20–24 July 1992; Wayman, C.M., Perkins, J., Eds.; Monterey Institute for Advanced Studies: Monterey, CA, USA, 1993; p. 141.
28. Shih, C.H.; Averbach, B.H.; Cohen, M. Some Characteristics of the Isothermal Martensitic Transformation. *Trans. AIME* **1955**, *203*, 183–187. [[CrossRef](#)]
29. Razumov, I.K.; Gornostyrev, Y.N.; Katsnelson, M.I. Towards the ab initio based theory of phase transformations in iron and steel. *Phys. Met. Metallogr.* **2017**, *118*, 362–388. [[CrossRef](#)]
30. Vasil'ev, A.N.; Bozhko, A.D.; Khovailo, V.V.; Dikshtein, I.E.; Shavrov, V.G.; Buchel'nikov, V.D.; Matsumoto, M.; Suzuki, S.; Takagi, T.; Tani J. Structural and magnetic phase transitions in shape-memory alloys  $\text{Ni}_{2+x}\text{Mn}_{1-x}\text{Ga}$ . *Phys. Rev. B* **1999**, *59*, 1113–1120. [[CrossRef](#)]
31. Heczko, O. Magnetic shape memory effect and highly mobile twin boundaries. *Mater. Sci. Technol.* **2014**, *30*, 1559–1578. [[CrossRef](#)]
32. Pareti, L.; Solzi, M.; Albertini, F.; Paoluzi, A. Giant entropy change at the co-occurrence of structural and magnetic transitions in the  $\text{Ni}_{2.19}\text{Mn}_{0.81}\text{Ga}$  Heusler alloy. *Eur. Phys. J. B* **2003**, *32*, 303–307. [[CrossRef](#)]
33. Hickel, T.; Uijttewaal, M.; Al-Zubi, A.; Dutta, B.; Crabowski, B.; Neugebauer, J. Ab Initio-Based Prediction of Phase Diagrams: Application to Magnetic Shape Memory Alloys. *Adv. Eng. Mater.* **2012**, *14*, 547–561 [[CrossRef](#)]
34. Dutta, B.; Cakir, A.; Giacobbe, C.; Al-Zubi, A.; Hickel, T.; Acet, M.; Neugebauer, J. Ab initio Prediction of Martensitic and Intermartensitic Phase Boundaries in Ni-Mn-Ga. *Phys. Rev. Lett.* **2016**, *116*, 025503. [[CrossRef](#)]
35. Sokolovskaya, Y.; Miroshkina, O.; Baigutlin, D.; Sokolovskiy, V.; Zagrebina, M.; Buchel'nikov, V.; Zayak, A.T. [[CrossRef](#)] A Ternary Map of Ni-Mn-Ga Heusler Alloys from Ab Initio Calculations. *Metals* **2021**, *11*, 973. [[CrossRef](#)]
36. Buchel'nikov, V.D.; Sokolovskiy, V.V.; Herper, H.C.; Ebert, H.; Gruner, M.E.; Taskaev, S.V.; Khovaylo, V.V.; Hucht, A.; Dannenberg, A.; Ogura, M.; et al. First-principles and Monte Carlo study of magnetostructural transition and magnetocaloric properties of  $\text{Ni}_{2+x}\text{Mn}_{1-x}\text{Ga}$ . *Phys. Rev. B* **2010**, *81*, 094411. [[CrossRef](#)]
37. Banik, S.; Ranjan, R.; Chakrabarti, A.; Bhardwaj, S. Structural studies of  $\text{Ni}_{2+x}\text{Mn}_{1-x}\text{Ga}$  by powder x-ray diffraction and total energy calculations. *Phys. Rev. B* **2007**, *75*, 104107. [[CrossRef](#)]

38. Righi, L. Neutron Diffraction Study of the Martensitic Transformation of Ni<sub>2.07</sub>Mn<sub>0.93</sub>Ga Heusler Alloy. *Metals* **2021**, *11*, 1749. [[CrossRef](#)]
39. Waske, A.; Dutta, B.; Teichert, N.; Weise, B.; Shayanfar, N.; Becker, A.; Hütten, A.; Hickel, T. Coupling Phenomena in Magnetocaloric Materials. *Energy Technol.* **2018**, *6*, 1429–1447. [[CrossRef](#)]
40. Buchelnikov, V.D.; Zayak, A.T.; Entel, P. Magnetoelastic phase transitions in cubic ferromagnets. *JMMM* **2002**, *242–245*, 1457–1459. [[CrossRef](#)]
41. Brown, P.J.; Bargawi, A.Y.; Crangle, J.; Neumann, K.U.; Ziebeck, K.R.A. Direct observation of a band Jahn-Teller effect in the martensitic phase transition of Ni<sub>2</sub>MnGa. *J. Phys. Condens. Matter* **1999**, *11*, 4715–4722. [[CrossRef](#)]
42. Uijttewaal, M.A.; Hickel, T.; Neugebauer, J.; Gruner, M.E.; Entel, P. Understanding the Phase Transitions of the Ni<sub>2</sub>MnGa Magnetic Shape Memory System from First Principles. *Phys. Rev. Lett.* **2009**, *102*, 035702. [[CrossRef](#)]
43. Zhang, Z.; James, R.D.; Muller, S. Energy barriers and hysteresis in martensitic phase transformations. *Acta Mater.* **2009**, *57*, 4332–4352. [[CrossRef](#)]
44. Kouvel, J.S. Specific Heat of a Magnetite Crystal at Liquid Helium Temperatures. *Phys. Rev.* **1956**, *102*, 1489–1490. [[CrossRef](#)]
45. Gruner, M.E.; Niemann, R.; Entel, P.; Pentcheva, R.; Roesler, U.K.; Nielsch, K.; Fahler, S. Modulations in martensitic Heusler alloys originate from nanotwin ordering. *Sci. Rep.* **2018**, *8*, 8489. [[CrossRef](#)] [[PubMed](#)]
46. Smart, J.S. *Effective Field Theories of Magnetism*; W.B. Saunders Company: Philadelphia, PA, USA; London, UK, 1966.

**Disclaimer/Publisher's Note:** The statements, opinions and data contained in all publications are solely those of the individual author(s) and contributor(s) and not of MDPI and/or the editor(s). MDPI and/or the editor(s) disclaim responsibility for any injury to people or property resulting from any ideas, methods, instructions or products referred to in the content.